Title

KINETIC STUDY OF ZIRCONIUM-IODINE REACTION BY MODULATED MOLECULAR BEAM MASS SPECTROMETRY

Authors

Balooch, M.
Olander, D.R.

Publication Date

1982-06-01

LBL-14518
Preprint

Lawrence Berkeley Laboratory
UNIVERSITY OF CALIFORNIA

Materials & Molecular Research Division

Submitted to Surface Science

KINETIC STUDY OF ZIRCONIUM-IODINE REACTION
BY MODULATED MOLECULAR BEAM MASS SPECTROMETRY

M. Balooch and D.R. Olander

June 1982

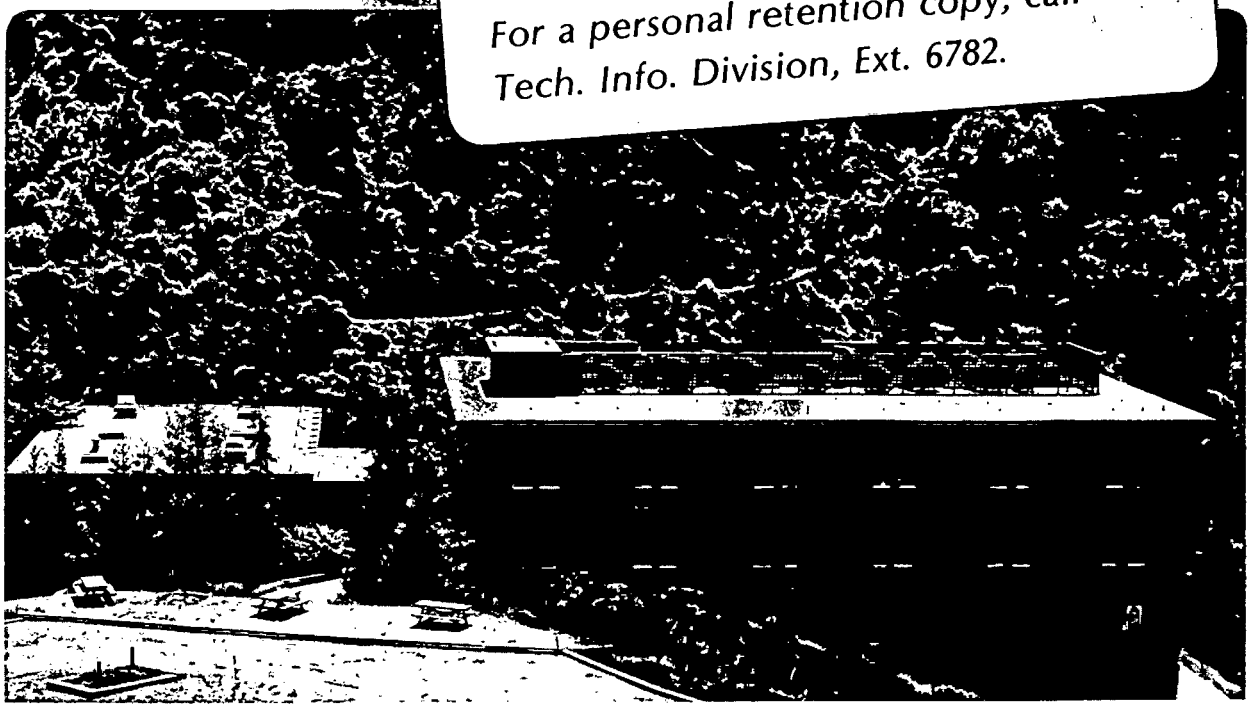

Prepared for the U.S. Department of Energy under Contract DE-AC03-76SF00098

DISCLAIMER

LBL-14518

KINETIC STUDY OF ZIRCONIUM-IODINE REACTION BY MODULATED MOLECULAR BEAM MASS SPECTROMETRY

By

M. BALOOCH AND D. R. OLANDER

Materials and Molecular Research Division of the
Lawrence Berkeley Laboratory, and the
Department of Nuclear Engineering
University of California
Berkeley, California 94720

This work was supported by the Director, Office of Energy Research. Office of Basic Energy Sciences, Materials Sciences Divison of the U.S. Department of Energy under contract #DE-AC03-76SF00098.

ABSTRACT

The reaction of molecular iodine with polycrystalline zirconium was studied by modulated molecular beam - mass spectrometric methods. The reaction was investigated in the temperature range 300 - 1330K and equivalent iodine pressures of 5×10^{-5} - 7×10^{-6} Torr. ZrI_4 was identified as the sole detectable reaction product at low temperatures (300-850K), achieving a maximum reaction probability at about 600K. At high temperatures, molecular dissociation and atomic desorption of iodine play a predominant role in the gas-surface reaction. The molecular beam data in conjunction with Auger and ESCA analysis of the surface after the experiment, support a reaction model involving a thin scale of a lower iodide present on the surface at low temperatures during the reaction. The kinetics of the reaction are governed by the diffusional properties and the reactivity of this scale with respect to adsorbed iodine atoms. At high temperatures the reaction mechanism consists of adsorption and dissociation of I_2 on the metal partially-covered with the iodide scale followed by desorption of atomic iodine.

I INTRODUCTION

It is generally believed that the failure of zirconium cladding in light water-cooled reactor (LWR) fuel elements is due to stress corrosion cracking (SCC) induced by one or more fission products(1,2). Iodine, an abundant fission product, has long been known to promote SCC of Zircaloy at reactor operating temperatures and is one of the prime suspects as the chemical substance involved in this type of cladding failure(2,3). Notwithstanding the controversial nature of the issue of iodine SCC in fuel elements(4), understanding of the chemistry of zirconium-iodine system is an essential part of the complex iodine-induced stress corrosion cracking mechanism. The thermochemical aspect of this problem has been considered in detail by Cubicciotti and co-workers and progress in this area is reported in several recent publications(5-8). Another aspect of the chemistry that needs further investigation is the kinetics of the reactions between iodine and zirconium, which is the subject of the present study.

In connection with the iodine refining of zirconium, several investigators(9-11), have investigated the kinetics of reaction of zirconium in the range 165-500°C and at iodine pressures of the order of a few Torr. Shelest el al.(11) have studied the effect of temperature and pressure on the rate of iodination of metallic zirconium using a quartz spiral balance. They found the overall order of the reaction to be 0.77 and an activation energy of $\sim$ 9 Kcal/mole. Busol(12) studied the rate of reaction of gaseous ZrI_4 with zirconium metal filings. He found the rate of disappearance of gaseous ZrI_4 to be parabolic with time in the temperature range of 600 to 800 K. Cubicciotti et al.(13) have also studied the formation of iodide products from reaction of Zr with gaseous ZrI_4

which they found to obey cubic kinetics.

In the present work, the kinetics of the zirconium-iodine system were investigated by modulated molecular beam techniques with temperature range of 300-1330K and equivalent iodine pressure of 5×10^{-5} - 7×10^{-6} Torr. A reaction mechanism was deduced by analysis of the amplitude and phase of the reaction product signals. The choice of a mechanism involving a lower iodide scale on the reacting surface was supported by post-reaction analysis of the metal surfaces by ESCA and Auger electron spectroscopy.

II EXPERIMENTAL

The molecular beam apparatus, which is a slightly modified version of one described previously(14), is shown in Fig. 1. It consists of three differentially-pumped chambers separated by collimating orifices. The source chamber contains the iodine molecular beam source and the chopper motor. This chamber is pumped by a 6 inch oil diffusion pump with the speed of 1500 lit/s. The iodine from a constant temperature bath is conducted through a heated tube to a small cell at the source tip where the temperature is controlled by a miniature furnace. The tube is kept at a slightly higher temperature than that of the reservoir to ensure that effusion from the system is controlled by reservoir temperature (and hence iodine pressure). The tube has an orifice with diameter of about 1 mm through which the molecular beam issues. The flux calculated from the reservoir temperature compares well with the flux obtained from pressure measurement and conductance of the line and the orifice.

The polycrystalline zirconium specimen is mounted on the end of a tube containing a filament which heats the target by radiation and by

electron bombardment. The surface temperature is measured by an infrared pyrometer. The specimen surface is 4 cm from the molecular beam source. The target chamber is pumped by a well-trapped 6 inch oil diffusion pump. A typical pressure of this chamber is $\sim 1 \times 10^{-9}$ Torr.

A portion of scattered iodine and reaction products are detected by a quadrupole mass spectrometer mounted in the detector chamber. The distance from the specimen surface to the mass spectrometer ionizer is 4 cm. This chamber is pumped by a 200 lit/s ion pump to about 1×10^{-10} Torr pressure.

The output from mass spectrometer is processed by a PAR HR-8 lock-in amplifier with a two-phase accessory to yield the first Fourier components of the periodic signals for the scattered reactant and desorbed products. The apparent reaction probability, ε (the ratio of the amplitudes of the product and reactant signals, corrected for ionization efficiences of the mass spectrometer) and phase lag, ϕ, which is the difference between the product and the reactant phase angles, are obtained from the information provided by the lock-in amplifier(15).

III RESULTS

Iodine was found to react vigorously with zirconium at temperatures below 1000 K. Zirconium-containing ions observed in the mass spectrometer were ZrI_3^+, ZrI_2^+, ZrI^+ and Zr^+. The signals at these masses all had the same phase and the same temperature dependence. The cracking pattern of a ZrI_4 beam scattered from zirconium target at room temperature matched that of the experimental reaction product fragments. Therefore, we concluded that the sole zirconium-bearing product of the reaction was ZrI_4. The atomic iodine signal detected at high temperature had to be extracted

from I^+ signals arising from ZrI_4 and I_2 cracking in the ionizer of the mass spectrometer. The experimental results of temperature, frequency and beam intensity variations on ε and ϕ are shown in Figs. 2-5. The curves on these graphs are best fits from the model discussed later.

Knowledge of the chemical state of the surface during bombardment by the iodine beam is essential for the development of a kinetic model. Cubicciotti and Scott(13) studied the reaction of zirconium with gaseous ZrI_4 in the temperature range 300-500°C and examined the solid zirconium iodides that formed on the zirconium surface by scanning electron microscopy. Initially isolated clusters of ZrI crystals formed which subsequently covered the whole surface. In a later stage a layer of diiodide was observed to form on the top of monoiodide. Further attack produced material of approximately the composition of ZrI_3 on the top surface.

Due to geometrical difficulties, we were unable to utilize Auger electron spectroscopy (AES) to monitor the surface in-situ while conducting the experiments. Attempts were made to analyze the surface by AES and ESCA in different chambers after an experiment, but iodine was not observed probably due to contamination by atmospheric gases during transfer. To avoid loss of an iodide scale during transport, the reaction surface at 580K was simultaneously coated with platinum supplied by a hot filament located in front of the target. Deposition was continued until the ZrI_4 signal was reduced to $\sim$ 10% of its initial value, which required approximately 20 monolayers of platinum. The sample was then removed and depth profile analyzed by ESCA and AES. The upper curve of Fig. 6 is the ESCA spectrum of the reacted surface which had not been protected by platinum. It shows oxygen and carbon lines from air exposure as well as zirconium peaks, but no iodine. Lower spectrum in fig. 6, after $\sim$ 20 Å sputtering, shows $\sim$ 2% iodine and 16% platinum on the surface. AES spectra of the

sample for three different sputter removal depths are shown in fig. 7. Although the peaks due to oxygen and iodine nearly coincide, they could be clearly resolved after removal of $\sim$ 100 Å of surface. These analyses confirm the existence of a nonvolatile iodide layer on the reacting surface. However, it was not possible to bury the iodide layer beneath a uniform coat of platinum, which would have permitted removal of the metal coat to expose an intact iodide scale amenable to analysis of the I/Zr ratio by ESCA or AES. First, by the co-impingement technique use to deposit the platinum during reaction, the metal coat was incorporated into the iodide scale. Second, platinum deposits on graphite in isolated patches at this temperature (16). If similar island deposition occurs on Zr, not all of the iodide scale is exposed at a definite sputter-removal depth.

In an attempt to investigate the effect of an oxidized surface on reaction, a beam of oxygen was directed at the target (600 K) along with a beam of iodine of intensity 5.6×10^{15} molecules/cm^2-s. No change in apparent reaction probability or phase lag of ZrI_4 was observed up to an intensity of $\sim 10^{16}$ oxygen molecules/cm^2-s striking the same spot as the iodine impingement. However, when the beam of iodine was turned off for about 10 minutes while the oxygen beam was on, no reaction product was detected when I_2 impingement was resumed. Then both beams were turned off and the sample was annealed in vacuum for 4 minutes at about 1200 K, after which the surface temperature was brought back to 600 K and the beam of iodine was turned on. The resulting reaction probability and phase lag of ZrI_4 are shown as triangles in Fig. 8. By repeating the 1200K heat treatment for another 7 minutes the magnitude of reaction probability and phase lag of ZrI_4 approached those characteristic of the

fresh zirconium surface (circles in Fig. 8). No oxyiodide was detected during these experiments. These tests demonstrated that the 1200 K annealing is sufficient to dissolve a thin oxide scale in the substrate metal. Partial dissolution evidently occurs in 4 minutes, and complete removal is accomplished in the second 7-minute treatment.

IV REACTION MECHANISM

The following observations serve as guidelines for construction of a kinetic model of the surface reactions:

1. An iodide scale is present on the zirconium surface during reaction at low temperatures. Although the I/Zr ratio of this scale could not be determined quantitatively by ESCA or AES, its presence is consistent with the observations of multiple scales with variable I/Zr ratios at I_2 pressures much higher than those used in the present work(13).

2. Figure 2 indicates that a distinct change in the reaction mechanism occurs at $\sim$ 850 K, where the signals of both I and ZrI_4 change precipitously. This behavior is best explained by the disappearance of the lower iodide scale from the surface at this temperature, and suggests that ZrI_4 is formed by I_2 reaction with the ZrI_x solid scale but that the bare metal which is present at high temperatures serves principally to dissociate impinging I_2.

3. The slow change of the phase lag of ZrI_4 with modulation frequency (Fig. 4) suggests that bulk diffusion, probably through the lower iodide scale on the surface, is an important step in the mechanism(15).

4. The reduction of the ZrI_4 reaction probability at temperatures below $\sim$ 500 K and the observation of phase lags larger than 90^o in the same temperature range (Fig. 2) indicates a mechanism consisting of series

steps prior to product desorption(15).

5. Production of ZrI_4 is linear in the reactant beam intensity while that of atomic iodine exhibits an apparent reaction order greater than unity (Fig. 3).

6. A minimum in the response of the iodine atom phase lag to modulation frequency (Fig. 5) is indicative of a branched process (i.e., two independent parallel paths(15)) for dissociating I_2 on the surface to form the atomic iodine product. A minimum in the atom phase lag is also observed when the temperature is varied (Fig. 2).

Low Temperature (T < 850 K)

The following reaction mechanism for surface temperatures below 850 K closely resembles that determined for the fluorine-tantalum system(14). The surface is assumed to be covered with a uniform scale of a lower iodide of zirconium. To simplify the analysis, the I/Zr ratio of the scale is assumed to be unity, corresponding to the lowest iodide of zirconium observed by Cubicciotti et al.(5-8). The elementary steps in the reaction model are:

$$I_2(g) \xrightarrow{r_1} 2I(ads) \qquad (1)$$

$$ZrI + I(ads) \xrightarrow{k_1} ZrI_2 \qquad (2a)$$

$$ZrI_2 + 2I(ads) \xrightarrow{fast} ZrI_4(ads) \qquad (2b)$$

$$I(ads) \underset{}{\overset{H}{\rightleftharpoons}} I(bulk, surface) \qquad (3)$$

$$I(bulk, surface) \xrightarrow{D} I(bulk, interface) \qquad (4)$$

$$I(bulk, interface) + Zr \xrightarrow{fast} ZrI \qquad (5)$$

$$ZrI_4(ads) \xrightarrow{k_2} ZrI_4(g) \qquad (6)$$

$$I(ads) \xrightarrow{k_3} I(g) \qquad (7)$$

The model contains no provision for evaporation of lower zirconium iodides or for surface recombination of I(ads) to form I_2. There is no experimental evidence for the formation of these products and application of the quasi-equilibrium model(17) to I_2 reaction with a ZrI_x surface ($1 < x < 2$) predicts only I and ZrI_4 as products.

Reaction (1) represents the dissociative chemisorption of molecular iodine on the surface of the ZrI scale exposed to the impinging reactant beam.

Reaction (2) represents the production of ZrI_4 by reaction between absorbed I atoms and the ZrI scale. The rate constant for production of ZrI_2 is denoted by k_1, which is assumed to be the limiting step in production of ZrI_4 on the surface. Addition of I atoms to ZrI_2 is assumed to be rapid.

Steps (3) - (5) provide a mechanism for regenerating the ZrI scale which is consumed at its upper surface by reaction (2). The adsorbed I atoms dissolve into the top surface of the scale with a solubility coefficient H (step (3)), then diffuse through the scale to the metal-scale interface (step (4)), where they rapidly and irreversibly react to form fresh scale (step (5)).

Reactions (6) and (7) account for the desorption of adsorbed ZrI_4 and I species. The rate constants for these reactions are denoted by k_2 and k_3. Reaction (6) could be a limiting step at low temperatures. As the surface temperature increases above $\sim$ 600 K, desorption of I(ads) (reaction (7)) causes a decrease in ZrI_4 production. In addition, diffusion in the scale demodulates the product signal and reduces its fundamental mode component, to which the detection system responds.

Numerical implementation of the kinetic model based on reactions (1) - (7) begins with determination of the thickness of the ZrI scale. At steady state, the rate at which the scale is removed by reaction (2) is equal to the rate at which it is produced by the combination of step (3) - (5). The thickness of the scale is(14):

$$\xi = \frac{DH}{k_1} \tag{8}$$

The balance on iodine atoms adsorbed on the ZrI scale is:

$$\frac{dm}{dt} = 2r_1 I_o\, g(t) - (3k_1 + k_3)m + D\left(\frac{\partial C}{\partial z}\right)_{z=0} \tag{9}$$

where m is the adsorbed iodine atom concentration, I_o is the iodine beam intensity and g(t) is the gating function of the beam. The first term on the right hand side of this equation represents the source of I atoms from the incident I_2 beam. The second term is the loss due to desorption of I atoms and production of ZrI_4. The last term on the right hand side represents loss of I atoms from the surface by solution and diffusion into the scale, where C is the concentration of iodine in the ZrI scale (in excess of the nominal $\frac{I}{Zr}$ ratio of unity). The diffusion coefficient of iodine atoms in the ZrI_4 scale is denoted by D.

Diffusion of iodine in the scale is governed by Fick's law:

$$\frac{\partial C}{\partial t} = D\,\frac{\partial^2 C}{\partial z^2} \tag{10}$$

where z is the coordinate perpendicular to the surface. The boundary condition at the scale/metal interface is:

$$C(z = \xi) = 0 \tag{11}$$

The second boundary condition can be expressed in terms of solubility coefficient, H, relating the surface concentration of I atoms to the bulk concentration of excess iodine in the upper surface of

of the scale:

$$C(z = 0) = H\,m \tag{12}$$

The mass balance on ZrI_4(ads), with concentration of p, is

$$\frac{dp}{dt} = k_1 m - k_2 p \tag{13}$$

To solve this system of equations for the first Fourier components of the product waveforms (which is what is measured experimentally), the following forms are assumed:

$$g = \tfrac{1}{2}(1 + g_1 e^{i\omega t}) \tag{14}$$

$$m = m_o + \bar{m}\, e^{i\omega t}$$

$$p = p_o + \bar{p}\, e^{i\omega t} \tag{15}$$

$$C = C_o + \bar{C}\, e^{i\omega t}$$

Eq(14) is the beam modulation function which is periodic with a frequency ω rad/s and $i = \sqrt{-1}$. In the representation of m, p and C by Eq(15), the quantities with subscript o arise from the steady component of the beam and the coefficients $\bar{m}$, $\bar{p}$ and $\bar{C}$ are complex quantities posessing amplitude and phase. Simultaneous solution of Eqs. (9), (10) and (13) results in the following reaction product vectors for ZrI_4 and I:

$$\varepsilon_{ZrI_4} e^{-i\phi_{ZrI_4}} = \frac{4k_2\bar{p}}{I_o g_1} = \frac{4\eta_1}{(1+i\,\frac{\omega}{k_2})\left[(3+\frac{k_2}{k_1}) + i\,\frac{\omega}{k_1} + \frac{\alpha DH}{k_1}\,\frac{1 + e^{-2\alpha\xi}}{1 - e^{-2\alpha\xi}}\right]} \tag{16}$$

and

$$\varepsilon_I e^{-i\phi_I} = \frac{k_3\bar{m}}{I_o g_1} = \frac{\eta_1}{i\frac{\omega}{k_3} + \left(1 + \frac{3k_1}{k_3}\right) + \frac{\alpha DH}{k_3}\,\frac{1 + e^{-2\alpha\xi}}{1 - e^{-2\alpha\xi}}} \qquad (17)$$

where

$$\alpha = \left(\frac{\omega}{D} i\right)^{\frac{1}{2}}$$

High Temperatures (T > 850 K)

At high temperature the ZrI scale breaks down to a partially-covered zirconium surface and a second route for producing atomic iodine, namely dissociation by the bare metal, becomes available. If this process is slower than I atom production and desorption on the remaining ZrI scale, a minimum in the phase lag variation with temperature can occur.

For zirconium partially covered with ZrI, the mechanism involves reactions (1) and (7) on the ZrI-covered portion surface and the following steps on the bare metal:

$$I_2(g) + 2Zr \xrightarrow{\eta_2} 2ZrI \qquad (18)$$

$$ZrI \xrightarrow{k_4} Zr + I(g) \qquad (19)$$

Reaction(18) represents dissociative chemisorption of molecular iodine followed immediately by reaction of the adsorbed I with zirconium to produce ZrI. The ZrI so formed decomposes with rate constant k_4. However, the balance between production of ZrI by reaction (18) and removal by reaction(19) results in a partial coverage of the surface by ZrI. Molecular iodine dissociatively adsorbs on and atomically desorbs from this portion of the surface with the same sticking probability and rate constant which characterize reactions (1) and (7) in the low-temperature mechanism. If the surface density of ZrI maintained by Eqs(18) and (19) is denoted by n molecules/cm^2 the fraction of the total surface covered by

this species is $n\sigma$, where σ is the projected area of a ZrI molecule. The adsorbed ZrI may be sufficiently surface-mobile to cluster into islands, leading to a discontinuously covered surface. The surface balance for ZrI is:

$$\frac{dn}{dt} = 2\,\eta_2\,I_o\,g(t)\,(1 - n\sigma) - k_4\,n \qquad (20)$$

The first term on the right hand side of Eq(20) represents the production of ZrI(ads) from I_2 gas striking the bare metal surface. The second term shows the loss of ZrI(ads) due to dissociation of this molecule, desorbing I and leaving Zr behind. The mass balance on adsorbed iodine atom (with surface concentration m) on ZrI clusters can be represented by:

$$\frac{dm}{dt} = 2\eta_1\,I_o\,g(t)\,(n\sigma) - k_3 m \qquad (21)$$

The first term on the right hand side of Eq (21) represents the rate of dissociative adsorption on ZrI(ads). The second term represents the loss of iodine atoms due to desorption. This equation is the same as Eq (9) in the limit where the coverage of ZrI is unity (i.e. $n\sigma \to 1$) and tetraiodide production and bulk solution-diffusion are negligible.

The reaction product vector for iodine atom production can be shown to be:

$$\varepsilon_I e^{-i\phi_I} = \frac{\eta_2(1 - \sigma n_o)}{\left(1 + \frac{\eta_2 I_o \sigma}{k_4}\right) + \frac{\omega}{k_4} i} + \frac{\sigma\eta_1 n_o + \frac{I_o\,\eta_1\sigma}{2k_4}\left\{\frac{\eta_2(1 - \sigma n_o)}{1 + \frac{\eta_2\,I_o\sigma}{k_4} + \frac{\omega}{k_4} i}\right\}}{1 + \frac{\omega}{k_3} i} \qquad (22)$$

where $$n_o = \frac{\eta_2 I_o}{k_4 + \eta_2 I_o \sigma} \qquad (23)$$

Curves representing the theoretical apparent reaction probabilities and phase lags of the products I and ZrI_4 are compared with the data in Figs. 2-5. Such comparison requires selection of all the physico-chemical parameters describing each elementary step of the model, which include the stiking probabilities η_1 and η_2, the rate constants k_1 - k_4, the solution/diffusion properties of the scale H and D, and the projected area of adsorbed ZrI, σ. The parameters H and D always appear as the product H^2D in the model and σ is estimated to be 1.6×10^{-15} cm^2 from the cross sections of iodine and zirconium atoms(18). Five parameters (k_1 - k_4, H^2D) are assumed to exhibit Arrhenius-type temperature dependences but the sticking probabilities are considered to be temperature-independent. Thus 12 parameters were obtained by fitting the model to the complete set of data in Figs. 2-5. The best values are chosen by an optimization routine which has been modified to accept complex numbers for comparing molecular beam data with the theoretical reaction model(19). The results are summarized in table 1.

VI DISCUSSION

The near-unity stiking probabilities of iodine on both ZrI and Zr are essential for the explanation of the vigorous reaction between iodine and zirconium.

The activation energy of the parameter k_3 represents desorption of iodine atom from ZrI scale. The value 50 kcal/mole shown in Table 1 compares satisfactorily with the value of 58 kcal/mole for equilibrium reaction(20):

$$ZrI_2(s) \longrightarrow ZrI(s) + I(g)$$

which closely resembles reaction (7).

The pre-exponential for desorption of I and ZrI_4 (k_2 and k_3) are consistent with vibrational frequences of adsorbed species. The low pre-exponential factor for formation of ZrI_2 and decomposition of ZrI(ads) (with rate constants of k_1, k_4) often characterize reaction-controlled surface steps(21).

Interpretation of the results with a model which assumes formation of lower iodide scale on the substrate is consistent with many observations of metal-halogen reactions. Early work by McKinley(22-24) demonstrates the existence of a scale on the reaction of nickel with bromine, chlorine and fluorine. The assumption of scale formation by Machiels and Olander(14) in the reaction between fluorine and tantalum was later confirmed by Nordine(25) in his study of the kinetics of fluorine reactions with iridium, platinum and tantalum using transonic flow reactor techniques. Another example of scale formation in low pressure halogen-metal reactions is the iron-chlorine system(26).

Because the molecular beam reaction response of the system depends only on the product H^2D while according to Eq.(8), the scale thickness requires knowledge of HD, the thickness of the scale cannot be determined from the model unless the diffusion coefficient of I in the scale or the solubility coefficient is known. Assuming $D = 10^{-15}$ cm^2/s at 600 K gives a scale thickness ξ = 10 Å, while for $D = 10^{-13}$ cm^2/s a thickness of 100 Å is predicted.

VII CONCLUSIONS

The model proposed for the low-pressure zirconium-iodine reaction is based on the formation of lower iodide scale on the surface. The

quantitative prediction based on the diffusion in scale provides a good fit to the molecular beam data and yields values of the rate constants of the elementary steps in the mechanism which appear to be reasonable.

Acknowledgement

This work was supported by the Director, Office of Energy Research, Office of Basic Energy Sciences, Materials Sciences Division of the U.S. Department of Energy under contract #DE-AC03-76SF00098.

TABLE 1 Parameters of the Zr-I_2 Surface Reaction

Parameter	Pre-exponential factor	Activation energy kcal/mole
η_1	1.0	-
η_2	0.8	-
k_1	1.6×10^{6} s^{-1}	15
k_2	1.4×10^{14} s^{-1}	24
k_3	1.7×10^{13} s^{-1}	50
k_4	1.7×10^{3} s^{-1}	13
H^2D	1.3×10^{10} s^{-1}	21

REFERENCES

1. J.H. Davies et al., in Proc. ANS Topical Meeting Water Reactor Fuel Performance, St. Charles, Illinois, May 9-11, 1977, p. 230.
2. J. T. A. Roberts, E. Smith, N. Fuhrman, and D. Cubicciotti, Nucl. Technol., 35, 131 (1977).
3. J. T. A. Roberts, "Structural Materials in Nuclear Power Systems", pp. 77-85, Plenum Press (1981).
4. D. R. Olander, to be published in J. of Nucl. Mater.
5. P. D. Kleinschmidt, D. Cubicciotti and D. L. Hildenbrand, J. Electrochem. Soc., 125 , 1543 (1978).
6. D. Cubicciotti, D. L. Hildenbrand, K. H. Lau and P. D. Kleinschmidt, "Thermodynamics of Zirconium Iodides at Elevated Temperatures", In D. L. Hildenbrand and D. Cubicciotti (eds.), High Temperature Metal Halide Chemistry, The Electrochemical Society, Princeton, New Jersey, 1978, p. 217.
7. D. Cubicciotti, K. H. Lau and M. J. Farrante, J. Electrochem. Soc., 125, 975 (1978).
8. D. Cubicciotti and K. H. Lau, J. Electrochem. Soc. 128, 196 (1981).
9. Z. M. Shapiro, "Iodide Decomposition Process for Production of Zirconium" In B. Lustman and F. Kerze (eds.), Metallurgy of Zirconium, McGraw-Hill, New York, 1955, Chap. 5.
10. R. M. Horton and R. L. Kinney, "Kinetics of Formation of ZrI_4 from Zr and I_2" - In Z. A. Foroulis and W.W. Smeltzer (eds.), Metal Slag Gas Reactions and Processes, The Electrochemical Society, Princeton, New Jersey, 1975, p. 317.
11. L. N. Shelest, E. K. Safronov and A. S. Mikhailova, Russ. J. Inorg. Chem., 18, 9 (1973).

12. F. I. Busol, Russ. J. Phys. Chem., 33, 799 (1959).

13. D. Cubicciotti and A. C. Scott, J. Less-Common Metals 77, 241 (1981).

14. A. J. Machiels and D. R. Olander, Surface Sci. 65, 325 (1977).

15. R. H. Jones, D. R. Olander, W. J. Siekhaus and J. A. Schwartz, J. Vacuum Sci. Technol. 9, 1429 (1972).

16. D. R. Olander and M. Balooch, J. Catalysis, 60, 41 (1979).

17. J. C. Batty and R. E. Stickney, J. Chem. Phys. 51, 4475 (1969).

18. J. B. Mann in "Recent Developments in Mass Spectroscopy", K. Ogata and T. Hayakawa (eds.), Baltimore, University Park Press, (1970), p. 814.

19. A. J. Machiels and D. R. Olander, High Temp. Sci., 9, 3 (1977).

20. D. Cubicciotti, R. L. Jones and B. C. Syrett, "Chemical Aspects of Iodine-Induced Stress Corrosion Cracking of Zircaloy", ASTM Fifth Conference on "Zirconium in Industry," (1980).

21. R. C. Baetzold and G. A. Somorjai, J. Catal. 45, 94 (1976).

22. J. D. McKinley, J. Chem. Phys. 40, 120 (1964).

23. J. D. McKinley, J. Chem. Phys. 40, 576 (1964).

24. J. D. McKinley, J. Chem. Phys. 45, 1690 (1966)

25. P. C. Nordine, J. Elect. Chem. Society, 125, 498 (1978).

26. M. Balooch, W. Siekhaus and D. R. Olander, to be published.

FIGURE CAPTIONS

1. Schematic of apparatus with iodine inlet system and oxygen doser.
2. Apparent reaction probabilities and phase lags of ZrI_4 and I as functions of zirconium target temperature.
3. Effect of beam intensity on the production of ZrI_4 and I at fixed temperature and modulation frequency.
4. Modulation frequency dependence of the ZrI_4 reaction probability and phase lag at fixed beam intensity and surface temperature.
5. Modulation frequency dependence of the atomic iodine reaction product vector at fixed beam intensity and surface temperature.
6. ESCA analysis of zirconium surface exposed to an iodine beam (upper spectrum) and of a zirconium surface coated with platinum during reaction with iodine (lower spectrum). 20 Å of the surface were removed by sputtering before recording the lower spectrum. Reaction with iodine and surface analysis were conducted in separate vacuum systems.
7. Auger electron spectra of a zirconium surface which had been platinum-coated during reaction with iodine and subsequently etched to depths of 4, 15 and 100 Å by sputtering. Reaction with iodine and surface analysis were conducted in separate vacuum systems.
8. Effect of annealing of a pre-oxidized zirconium specimen at 1200 K on ZrI_4 production at 600 K; 4 minute anneal (triangles) and an additional 7 minute anneal (circles).

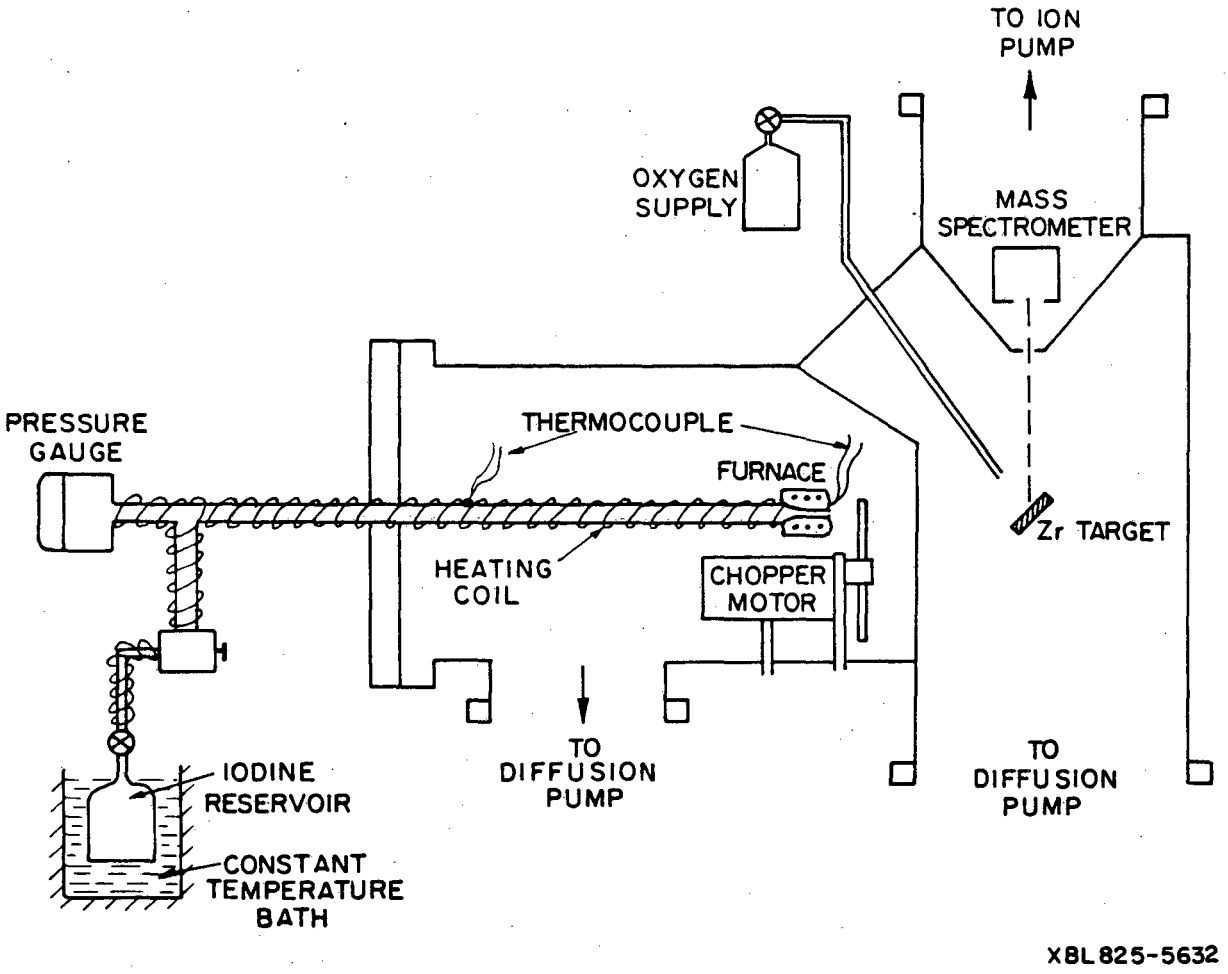
TO ION PUMP
OXYGEN SUPPLY
MASS SPECTROMETER
PRESSURE GAUGE
THERMOCOUPLE
FURNACE
Zr TARGET
HEATING COIL
CHOPPER MOTOR
TO DIFFUSION PUMP
TO DIFFUSION PUMP
IODINE RESERVOIR
CONSTANT TEMPERATURE BATH
XBL825-5632

Figure 1.

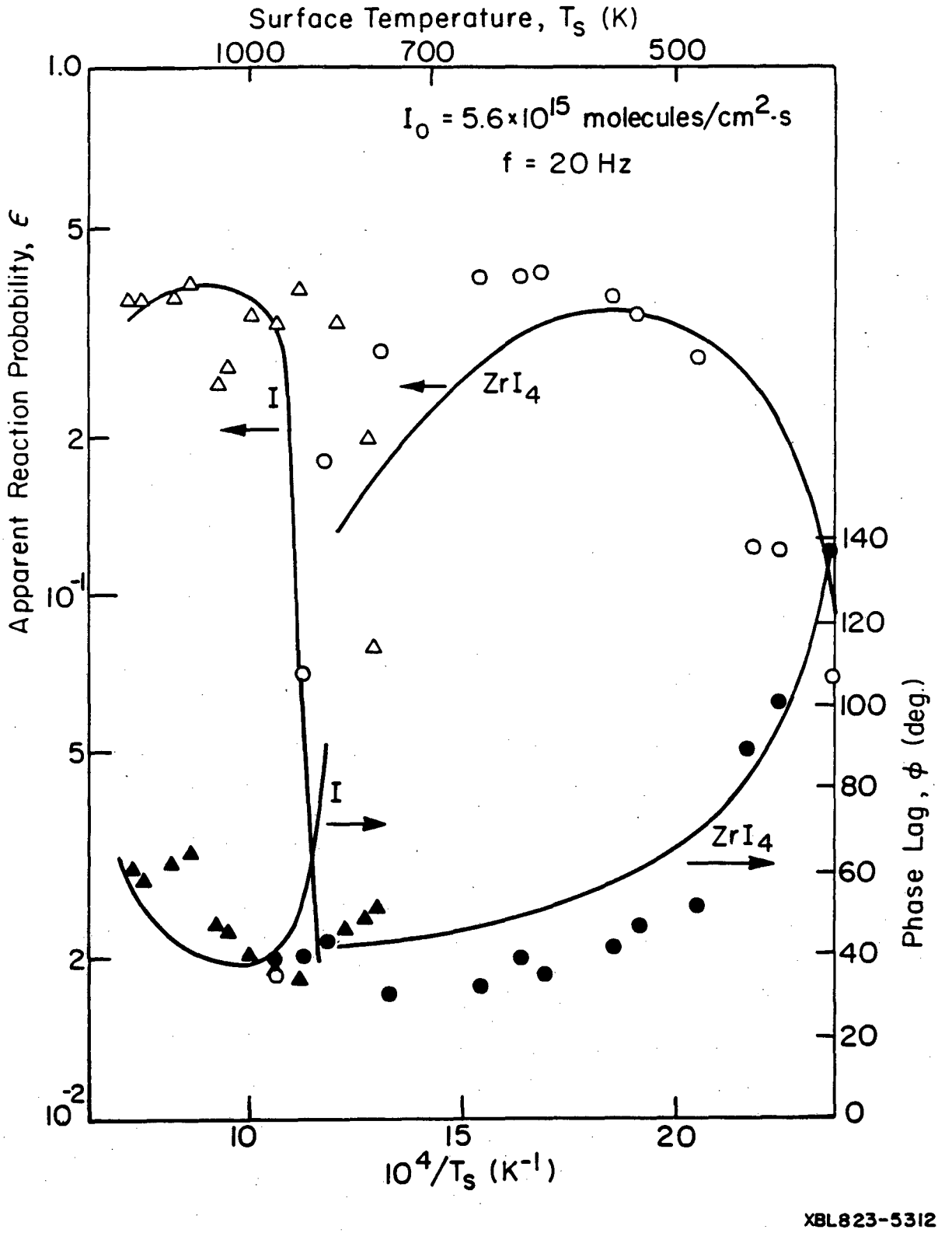
Surface Temperature, T_s (K)
1000
700
500
1.0
$I_0 = 5.6 \times 10^{15}$ molecules/cm^2-s
f = 20 Hz
Apparent Reaction Probability, ϵ
5
2
10^{-1}
5
2
10^{-2}
I
ZrI_4
I
ZrI_4
140
120
100
80
60
40
20
0
Phase Lag, ϕ (deg.)
10
15
20
$10^4/T_s$ (K^{-1})
XBL823-5312

Figure 2.

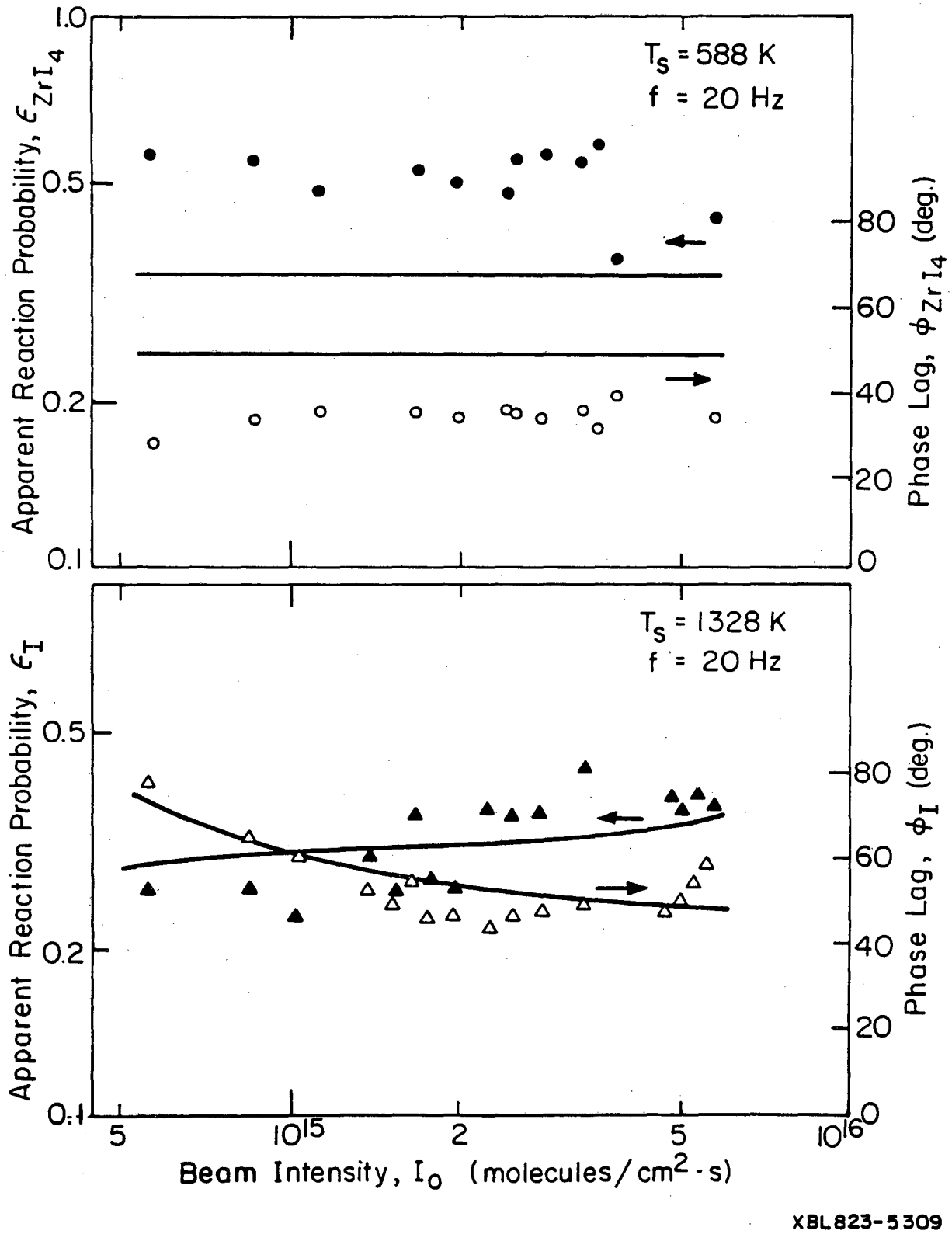
1.0
0.5
0.2
0.1
Apparent Reaction Probability, ϵ_{ZrI_4}
T_s = 588 K
f = 20 Hz
80
60
40
20
0
Phase Lag, ϕ_{ZrI_4} (deg.)
T_s = 1328 K
f = 20 Hz
Apparent Reaction Probability, ϵ_I
Phase Lag, ϕ_I (deg.)
5
10^{15}
2
5
10^{16}
Beam Intensity, I_o (molecules/cm^2 · s)
XBL823-5309

Figure 3.

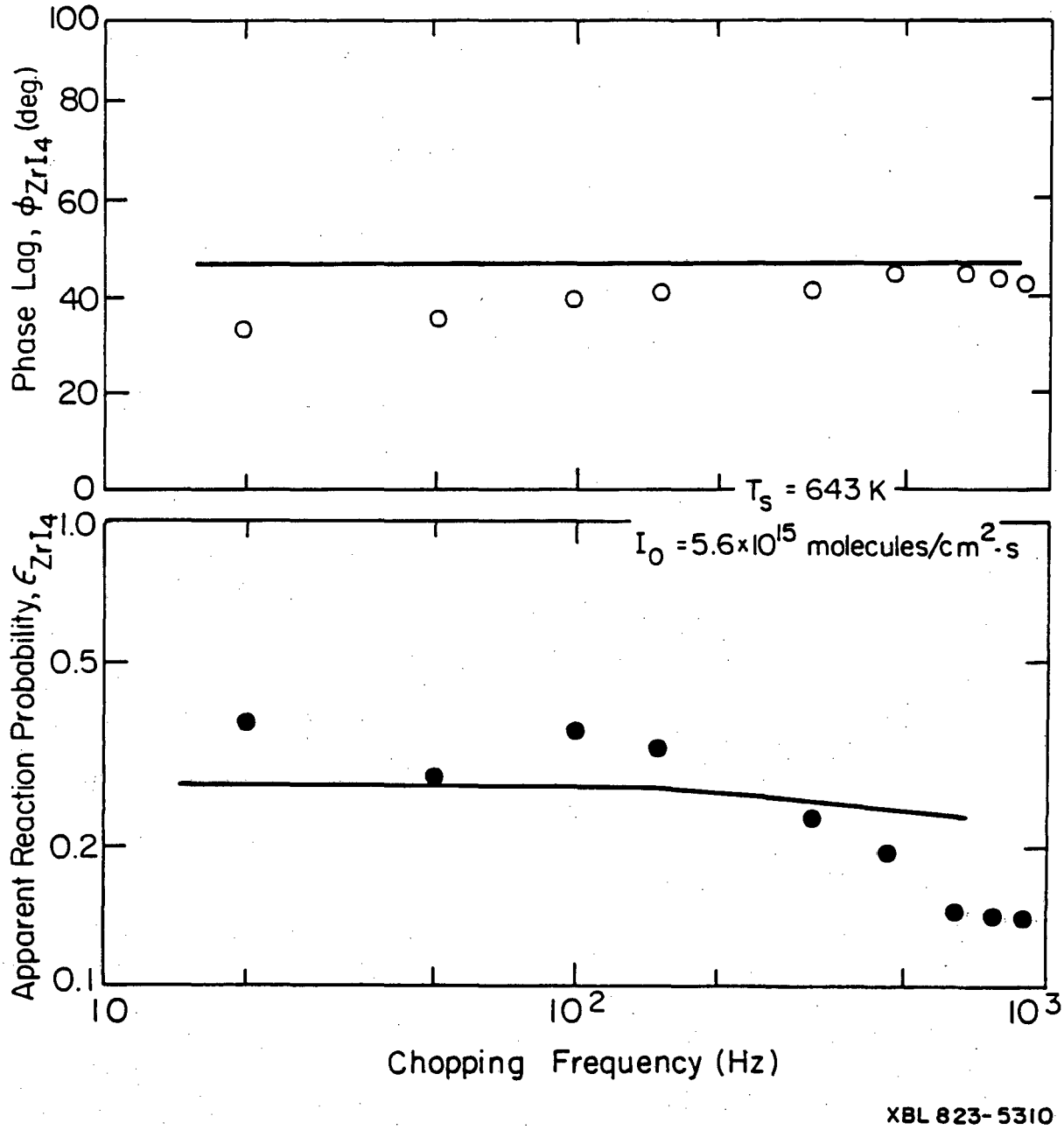
100
80
60
40
20
0
Phase Lag, ϕ_{ZrI_4} (deg.)
T_s = 643 K
I_0 = 5.6x10^{15} molecules/cm^2-s
1.0
0.5
0.2
0.1
Apparent Reaction Probability, ϵ_{ZrI_4}
10
10^2
10^3
Chopping Frequency (Hz)
XBL 823-5310

Figure 4.

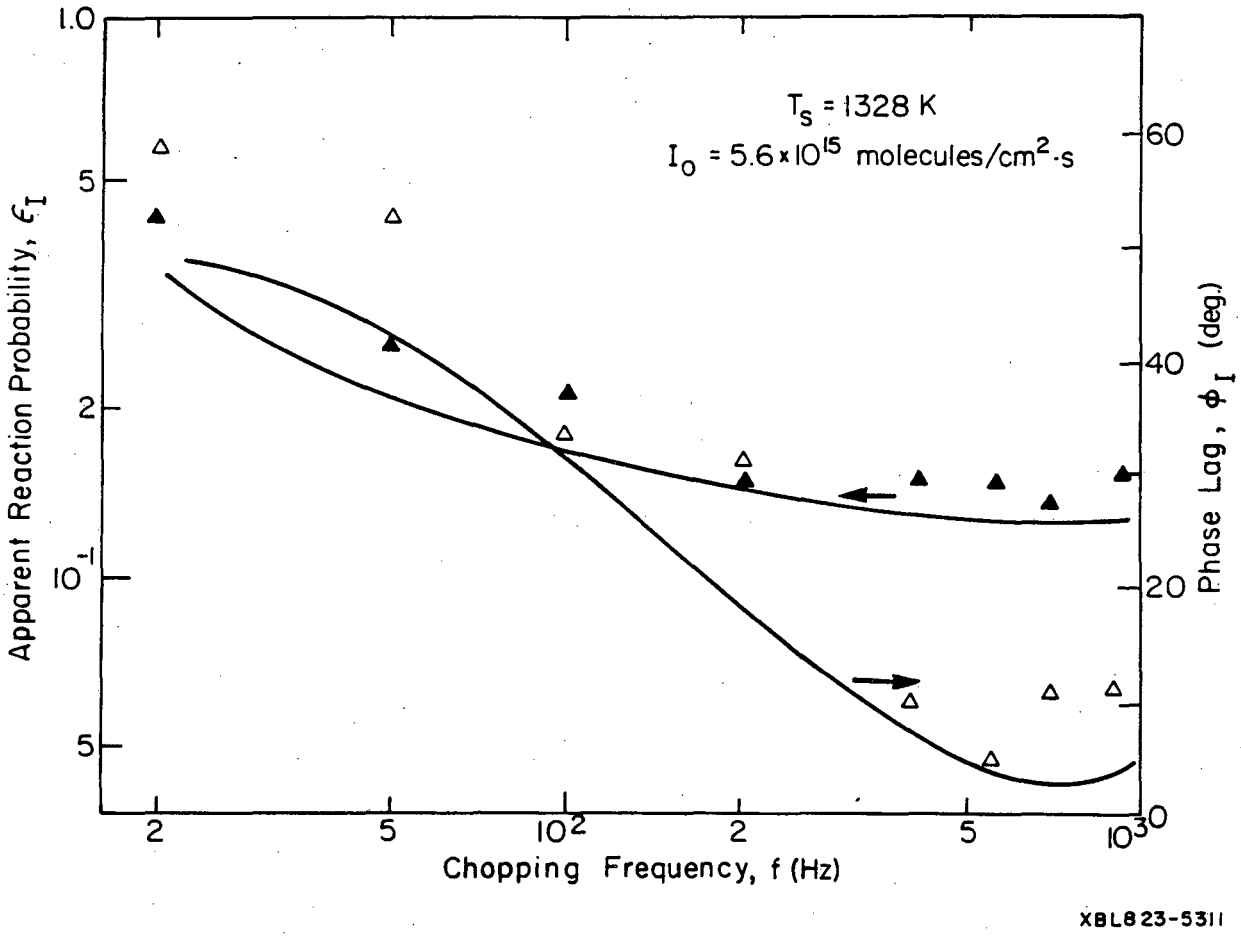
1.0
5
2
10^{-1}
5
Apparent Reaction Probability, ϵ_I
T_s = 1328 K
I_0 = 5.6 x 10^{15} molecules/cm^2·s
60
40
20
0
Phase Lag, ϕ_I (deg.)
2
5
10^2
2
5
10^3
Chopping Frequency, f (Hz)
XBL823-5311

Figure 5.

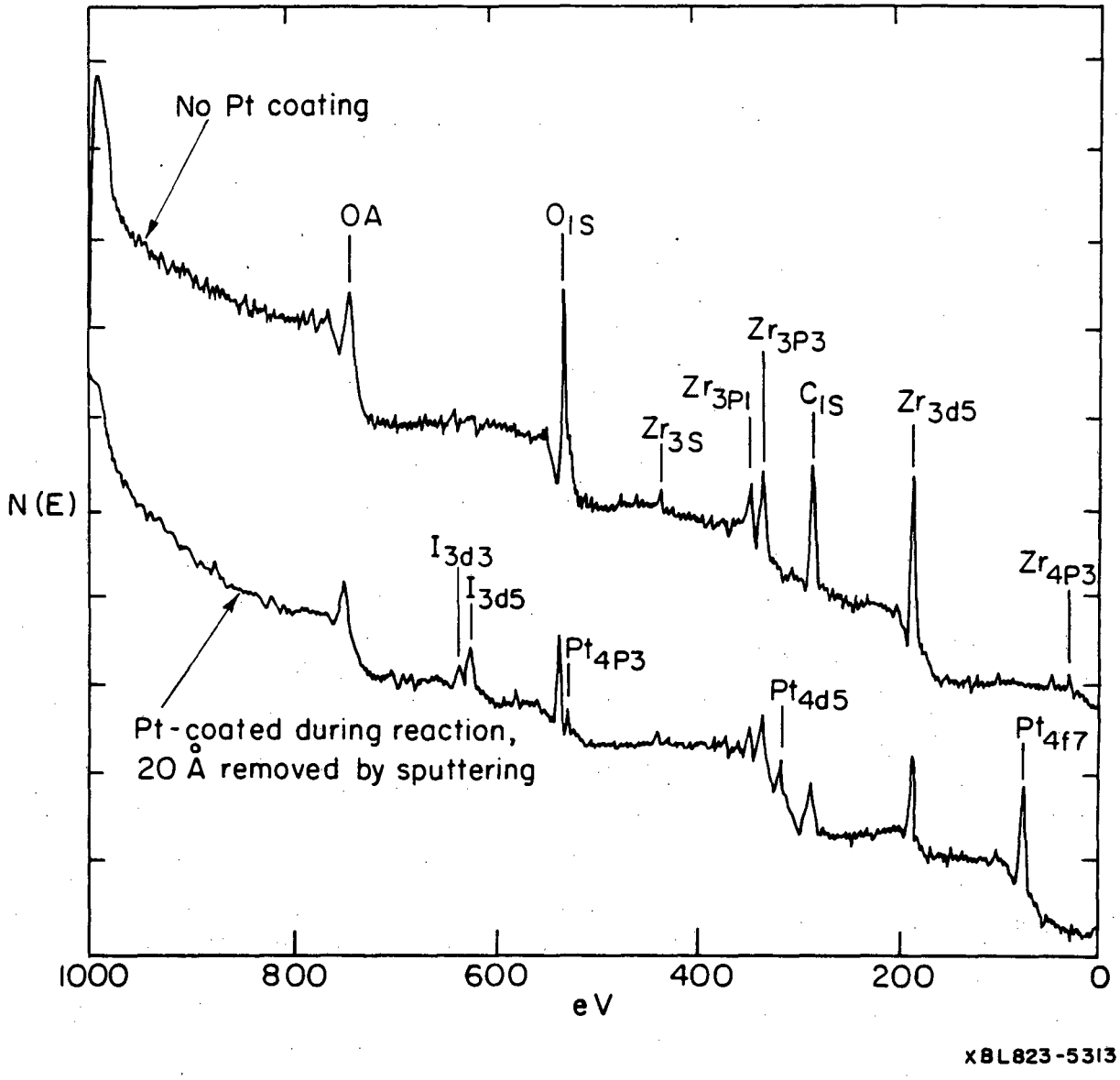
No Pt coating
OA
O1S
Zr3P3
Zr3P1
C1S
Zr3d5
Zr3S
N(E)
I3d3
I3d5
Zr4P3
Pt4P3
Pt4d5
Pt4f7
Pt-coated during reaction,
20 Å removed by sputtering
1000
800
600
400
200
0
eV
XBL823-5313

Figure 6.

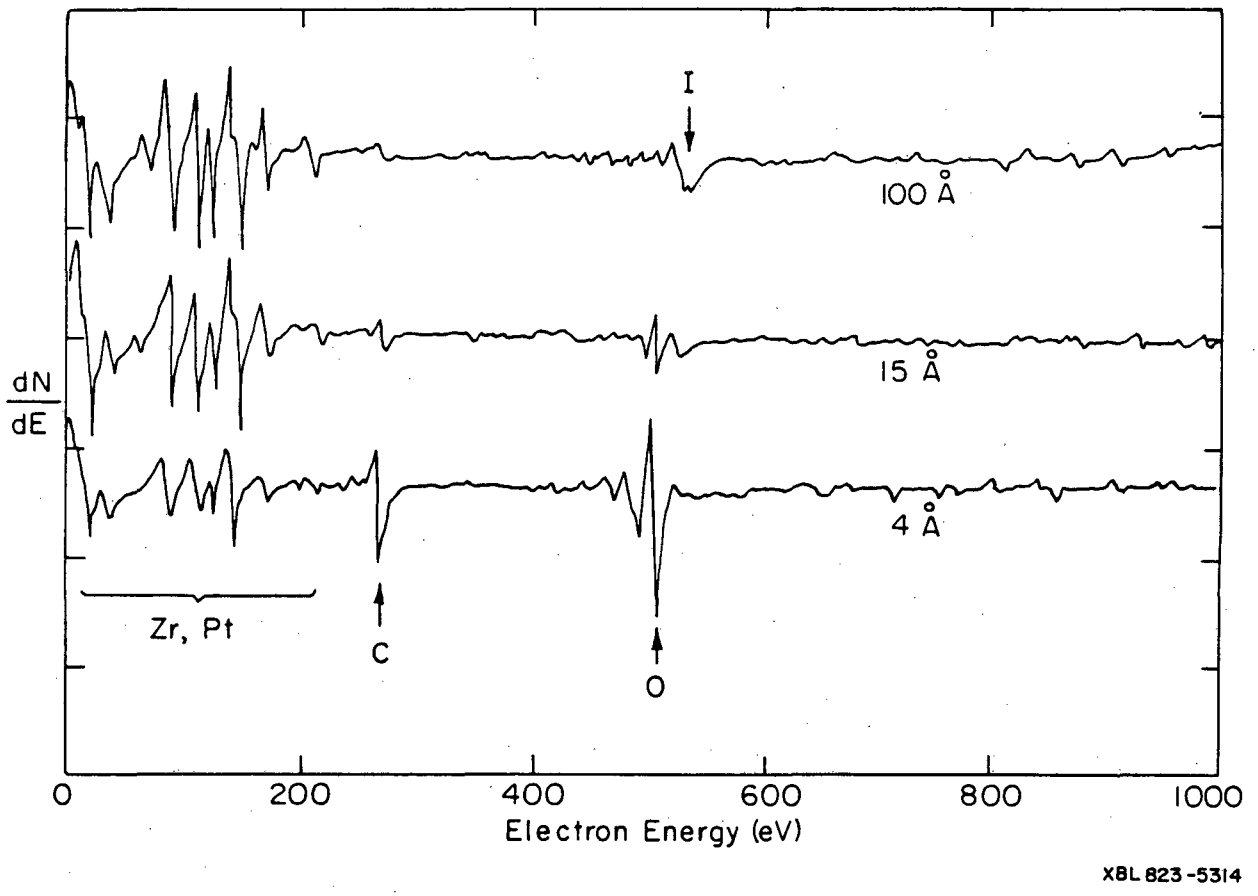
I
100 Å
15 Å
4 Å
dN
dE
Zr, Pt
C
O
0
200
400
600
800
1000
Electron Energy (eV)
XBL 823-5314

Figure 7.

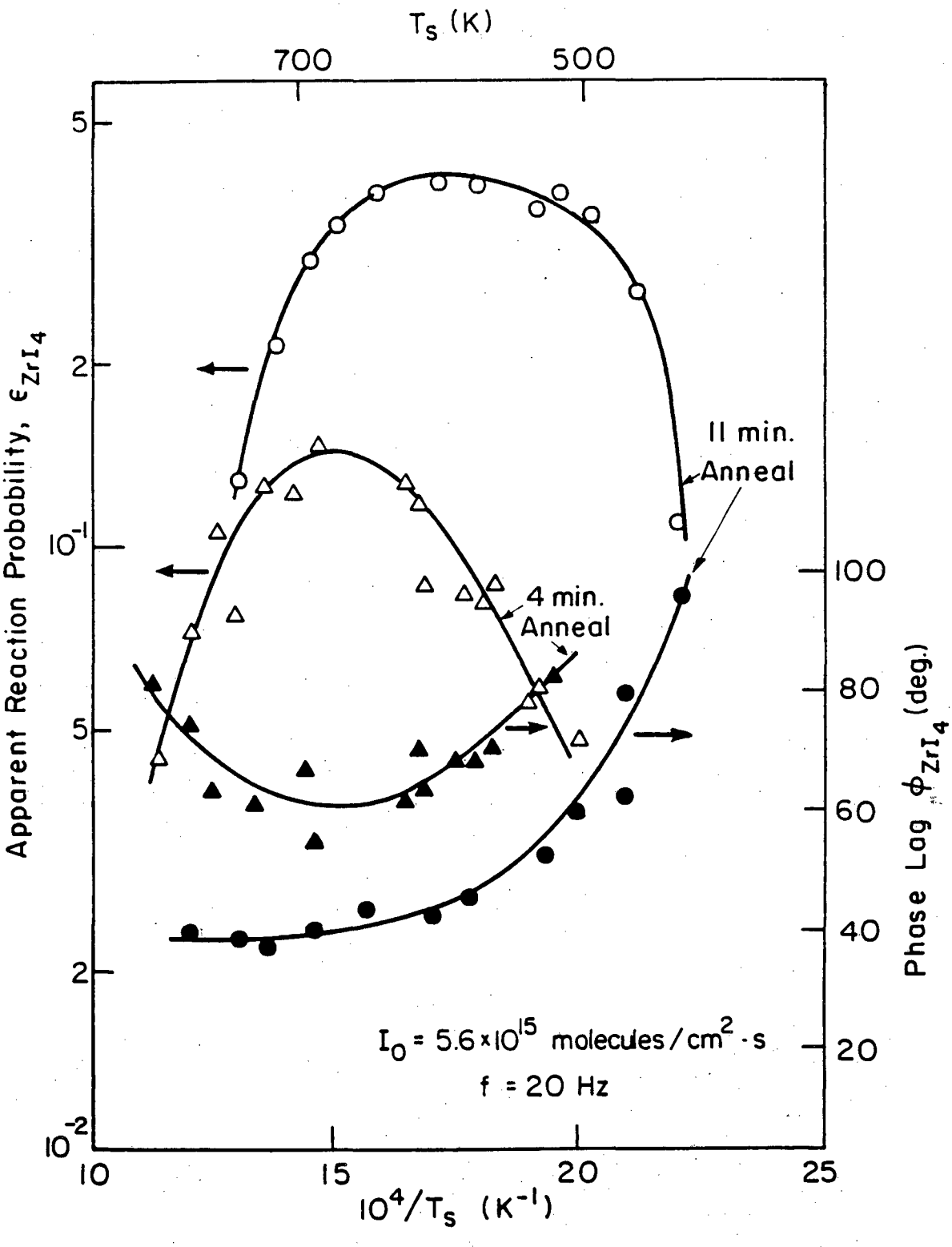
T_s (K)
700
500
5
2
10^{-1}
5
2
10^{-2}
Apparent Reaction Probability, ϵ_{ZrI_4}
11 min.
Anneal
4 min.
Anneal
$I_0 = 5.6 \times 10^{15}$ molecules/cm^2 · s
f = 20 Hz
100
80
60
40
20
Phase Lag ϕ_{ZrI_4} (deg.)
10
15
20
25
$10^4/T_s$ (K^{-1})
XBL 825-5631

Figure 8.

This report was done with support from the Department of Energy. Any conclusions or opinions expressed in this report represent solely those of the author(s) and not necessarily those of The Regents of the University of California, the Lawrence Berkeley Laboratory or the Department of Energy.

Reference to a company or product name does not imply approval or recommendation of the product by the University of California or the U.S. Department of Energy to the exclusion of others that may be suitable.

TECHNICAL INFORMATION DEPARTMENT
LAWRENCE BERKELEY LABORATORY
UNIVERSITY OF CALIFORNIA
BERKELEY, CALIFORNIA 94720